

- Aris-Brosou, S., and Z. Yang. 2002. Effects of models of rate evolution on estimation of divergence dates with special reference to the metazoan 18S ribosomal RNA phylogeny. *Syst. Biol.* 51:703–714.
- Aris-Brosou, S., and Z. Yang. 2003. Bayesian models of episodic evolution support a late precambrian explosive diversification of the metazoa. *Mol. Biol. Evol.* 20:1947–1954.
- Ayala, F. J., A. Rzhetsky, and F. J. Ayala. 1998. Origin of the metazoan phyla: Molecular clocks confirm paleontological estimates. *Proc. Natl. Acad. Sci. USA* 95:606–611.
- Barraclough, T. G., A. P. Vogler, and P. H. Harvey. 1998. Revealing the factors that promote speciation. *Philos. Trans. R. Soc. Lond. B* 353:241–249.
- Bromham, L. D., and B. M. Degnan. 1999. Hemichordates and deuterostome evolution: Robust molecular phylogenetic support for a hemichordate + echinoderm clade. *Evol. Dev.* 1:166–171.
- Bromham, L. D., and M. D. Hendy. 2000. Can fast early rates reconcile molecular dates with the Cambrian explosion? *Proc. R. Soc. Lond. B* 267:1041–1047.
- Bromham, L., and D. Penny. 2003. The modern molecular clock. *Nat. Rev. Genet.* 4:216–224.
- Bromham, L., A. Rambaut, R. Fortey, A. Cooper, and D. Penny. 1998. Testing the Cambrian explosion hypothesis by using a molecular dating technique. *Proc. Natl. Acad. Sci. USA* 95:12386–12389.
- Carlin, B. P., and T. A. Louis. 2000. Bayes and empirical Bayes methods for data analysis, 2nd Ed. Chapman and Hall, London.
- Cutler, D. J. 2000. Estimating divergence times in the presence of an overdispersed molecular clock. *Mol. Biol. Evol.* 17:1647–1660.
- Douzery, E. J. P., F. Delsuc, M. J. Stanhope, and D. Huchon. 2003. Local molecular clocks in three nuclear genes: Divergence times for rodents and other mammals and incompatibility among fossil calibrations. *J. Mol. Evol.* 57:S201–S213.
- Felsenstein, J. 2004. *Inferring phylogenies*. Sinauer Associates, Sunderland, Massachusetts.
- Holder, M., and P. O. Lewis. 2003. Phylogenetic estimation: Traditional and Bayesian approaches. *Nat. Rev. Genet.* 4:275–284.
- Huelsenbeck, J. P., B. Larget, and D. Swofford. 2000. A compound Poisson process for relaxing the molecular clock. *Genetics* 154:1879–1892.
- Huelsenbeck, J. P., F. Ronquist, R. Nielsen, and J. P. Bollback. 2001. Bayesian inference of phylogeny and its impact on evolutionary biology. *Science* 294:2310–2314.
- Kishino, H., J. L. Thorne, and W. J. Bruno. 2001. Performance of a divergence time estimation method under a probabilistic model of rate evolution. *Mol. Biol. Evol.* 18:352–361.
- Langley, C. H., and W. M. Fitch. 1974. An estimation of the constancy of the rate of molecular evolution. *J. Mol. Evol.* 3:161–177.
- Lynch, M. 1999. The age and relationships of the major animal phyla. *Evolution* 53:319–325.
- Nee, S., R. M. May, and P. H. Harvey. 1994. The reconstructed evolutionary process. *Phil. Trans. R. Soc. B* 344:305–311.
- Nielsen, C. 1995. *Animal evolution: Interrelationships of the living phyla*. Oxford University Press, Oxford.
- Orme, C. D. L., D. L. J. Quicke, J. M. Cook, and A. Purvis. 2002. Body size does not predict species richness among the metazoan phyla. *J. Evol. Biol.* 15:235–247.
- Pérez-Losada, M., J. T. Hoeg, and K. A. Crandall. 2004. Unravelling the evolutionary radiation of the Thoracian barnacles using molecular and morphological evidence: A comparison of several divergence time estimation procedures. *Syst. Biol.* 53:244–264.
- Peterson, K. J., J. B. Lyons, K. S. Nowak, C. M. Takacs, M. J. Wargo, and M. A. McPeck. 2004. Estimating metazoan divergence times with a molecular clock. *Proc. Natl. Acad. Sci. USA* 101:6536–6541.
- Sanderson, M. J. 1997. A nonparametric approach to estimating divergence times in the absence of rate constancy. *Mol. Biol. Evol.* 14:1218–1231.
- Sanderson, M. J. 2002. Estimating absolute rates of molecular evolution and divergence times: A penalized likelihood approach. *Mol. Biol. Evol.* 19:101–109.
- Smith, A. B., and K. J. Peterson. 2002. Dating the time of origin of major clades: Molecular clocks and the fossil record. *Annu. Rev. Earth Pl. Sci.* 30:65–88.
- Thorne, J. L., H. Kishino, and I. S. Painter. 1998. Estimating the rate of evolution of the rate of molecular evolution. *Mol. Biol. Evol.* 15:1647–1657.
- Weiss, R. E., and C. R. Marshall. 1999. The uncertainty in the true end point of a fossil's stratigraphic range when stratigraphic sections are sampled discretely. *Math. Geol.* 31:435–453.
- Wray, G. A., J. S. Levinton, and L. H. Shapiro. 1996. Molecular evidence for deep precambrian divergences among metazoan phyla. *Science* 274:568–573.
- Yang, Z., and B. Rannala. 1997. Bayesian phylogenetic inference using DNA sequences: A Markov chain Monte Carlo method. *Mol. Biol. Evol.* 14:717–724.
- Yoder, A. D., and Z. Yang. 2000. Estimation of primate speciation dates using local molecular clocks. *Mol. Biol. Evol.* 17:1081–1090.
- Zhang, J., and X. Gu. 1998. Correlation between the substitution rate and rate variation among sites in protein evolution. *Genetics* 149:1615–1625.

First submitted 1 July 2004; reviews returned 3 October 2004;  
final acceptance 5 November 2004  
Associate Editor: Frank Anderson

## Distances and Directions in Multidimensional Shape Spaces: Implications for Morphometric Applications

CHRISTIAN PETER KLINGENBERG<sup>1</sup> AND LEANDRO R. MONTEIRO<sup>2</sup>

<sup>1</sup>Faculty of Life Sciences, The University of Manchester, Michael Smith Building, Oxford Road, Manchester M13 9PT, United Kingdom;  
E-mail: cpk@manchester.ac.uk

<sup>2</sup>Laboratório de Ciências Ambientais, Centro de Biociências e Biotecnologia, Universidade Estadual do Norte Fluminense, Avenida Alberto Lamego 2000, Parque Califórnia, Campos dos Goytacazes, 28013-600, Rio de Janeiro, Brasil;  
E-mail: lrmont@uenf.br

The methods of geometric morphometrics, which combine an explicitly geometric definition of shape with the flexible tools of multivariate statistics, have become established in the past decade as the “morphometric

synthesis” (Bookstein, 1996, 1998). Considerable effort is now directed at applying these methods in diverse biological contexts. Therefore, the morphometric methods need to be linked to the experimental protocols and

statistical frameworks that underlie diverse applications such as phylogenetic comparative analyses (Rohlf, 2001, 2002) or quantitative genetics (Klingenberg and Leamy, 2001; Monteiro et al., 2002). Morphometric analyses provide tools for answering specific questions that depend on the context of each particular study. Statistical tests and predictions of effects usually can make use of the existing theory for the application, whereas the interpretation and graphical display of effects are specific to geometric morphometrics.

Precisely how the morphometric methods should be adapted to different biological contexts has provoked vigorous debate. An issue that has attracted particular attention is how to implement linear statistical models in geometric morphometrics. Should the inferred effects of experimental or observational factors on shape be considered exclusively in their absolute magnitude, using the Procrustes metric that is at the core of geometric morphometrics (e.g., Bookstein, 1996)? Or alternatively, is it legitimate, depending on context, to consider the effects considered relative to the observed variation as in standard multivariate analysis of variance and related statistical procedures?

The controversy has focused on several specific issues that are aspects of this question. Most recently, the debate has been conducted on the Morphmet E-mail list (February 2004; archive available at <http://www.mail-archive.com/morphmet@wfubmc.edu/>) as well as in a published exchange on quantitative genetics of shape (Klingenberg, 2003b; Monteiro et al., 2003). One position is that some of the standard analyses of multivariate statistics are inherently incompatible with morphometrics. For example, Bookstein (1991: 114) stated "Discriminant-function analysis is not a morphometric technique . . ." and added "Neither is the extension to multiple groups, canonical-variates analysis." This position is controversial because canonical variate analysis is one of the most frequently used techniques in morphometrics (e.g., Rohlf et al., 1996; Duarte et al., 2000; Corti and Rohlf, 2001; Douglas et al., 2001; Rüber and Adams, 2001; Dobigny et al., 2002; Cardini, 2003; Debat et al., 2003; Harvati, 2003; Klingenberg et al., 2003a).

Here we provide a general discussion of the problem, and we apply these considerations in two different examples of biological applications. In the first example, we extend and clarify an earlier debate about the application of geometric morphometrics to quantitative genetics (Klingenberg and Leamy, 2001; Monteiro et al., 2002; Klingenberg, 2003b; Monteiro et al., 2003). In the second example, we use the logic of transformed shape spaces in a different context to define a new measure of individual asymmetry of shape as an alternative to those suggested by Klingenberg and McIntyre (1998) and Palmer and Strobeck (2003).

#### SHAPE VARIATION

Shape is defined mathematically as all the geometric information about an object except for its size, position, and orientation or, in other words, all those properties that are invariant to scaling, translation, and rotation

(e.g., Bookstein, 1991: 126, 180; Dryden and Mardia, 1998: 1). This definition is used throughout geometric morphometrics and is applicable both to configurations of landmarks and to outline contours of objects. Because multiple geometric features are required to characterize the shape even of very simple figures, shape is an inherently multidimensional phenotype.

The shapes of landmark configurations can be represented as points in a shape tangent space (e.g., Dryden and Mardia, 1998; Rohlf, 1999), within which the methods of multivariate statistics can be used. Differences between pairs of shapes or deviations of individual shapes from the population average can be characterized by their magnitude, measured as a Procrustes distance, and their direction in the tangent space. As long as the complete information about shape is entered in the analysis, it does not matter whether the shape variables used are the complete set of partial warp scores and uniform components or the coordinates of Procrustes-aligned landmarks projected onto the tangent space. Both these sets of variables describe the same variation, and one can be transformed into the other by a rotation of the coordinate system (e.g., Rohlf, 1999: 214).

A key characteristic of geometric morphometrics is that points in the shape tangent space can be related back to actual shapes in the original plane or three-dimensional space of the landmark coordinates. Likewise, vectors in the shape tangent space correspond to shape changes. This relationship between the shape tangent space and the physical space in which the configurations were digitized makes it possible to visualize directly the results of statistical analyses. Maintaining these relationships imposes some restrictions on the mathematical operations that can be used in morphometrics, because some transformations destroy the special properties of shape tangent space and the direct link to the original landmark configurations.

A substantial body of mathematical theory has been developed for the special case when shape variation is isotropic, that is, when each landmark is equally variable, the variation at each landmark is the same in all directions, and variation is independent among landmarks (e.g., Goodall, 1991; Dryden and Mardia, 1998). This means that the scatter of landmark positions around the sample average is circular, with the same spread at each landmark. Although this model is convenient because it greatly simplifies the statistical analysis of shape variation, isotropic variation is rarely found in biological data sets. To the contrary, landmarks usually differ in their amounts of variation, they show a clear directionality of variation, and usually there exist associations between the landmarks. These deviations from the isotropic condition are often the very subject of interest, for instance, in studies of morphological integration (Klingenberg and McIntyre, 1998; Badyaev and Foresman, 2000; Debat et al., 2000; Klingenberg and Zaklan, 2000; Klingenberg et al., 2001a, 2003b, 2004; Bookstein et al., 2003). Accordingly, it is important to take into account the nonisotropic nature of shape variation.

To adjust for this, many of the standard methods of multivariate statistics use transformations of the data space.

The Procrustes approach has been criticized because it can produce estimates that are statistically inconsistent if variation is not isotropic (Lele, 1993; a critique repeated by Lele and Richtsmeier, 2001: 94). Kent and Mardia (1997) confirmed that statistical inconsistency can occur if the ratio of signal to noise goes toward zero (i.e., if the error distribution is large relative to the dispersion of the landmark positions in the mean form). They pointed out, however, that this problem does not apply if the data are tightly clustered around the mean shape (Kent and Mardia, 1997: 286), as is the case in the vast majority of biological examples, particularly in studies at the intraspecific level or in comparisons among closely related species. Similarly, Dryden and Mardia (1998: 287) emphasize that for small amounts of shape variation, the Procrustes methods and distance-based alternatives such as EDMA (championed by Lele and Richtsmeier, 2001) will produce shape coordinates that are effectively linear transformations of each other. After a transformation of those spaces as we discuss them in this paper, the different approaches will therefore produce virtually the same statistical results, and will differ primarily in the form of presentation. Dryden and Mardia (1998: 287) further suggest a rule of thumb that if the full Procrustes distances between the average shape and all the specimens are less than about 0.2, all methods yield very similar results. This is a far greater amount of shape variation than is usually found in morphometric data sets.

#### TRANSFORMATIONS OF MULTIVARIATE SPACES

Imagine a data set consisting of three groups arranged in a two-dimensional space (a plane, which might be the shape tangent space for a triangle of landmarks) so that the points corresponding to the three group means form an equilateral triangle (Fig. 1A). By definition, these three groups are at equal distances from each other. Despite the equal distances between means, however, the three groups in Figure 1A are not equally distinct from each other because the variation within groups is not isotropic. Groups 1 and 2, for which the mean difference is nearly aligned with the axis of greatest within-group variation, are almost overlapping. In contrast, group 3 is clearly separate from either one of the others, as the mean differences are roughly perpendicular to the axis of greatest within-group variation. This example shows that the distinctness of groups depends not only on the distance between group means, but also on the direction of the mean difference relative to the directionality of variation within groups. In contrast, if the variation within groups is isotropic, the degree of separation depends only on the distances between means (Fig. 1B).

If variation is nonisotropic, the task of discriminating between groups can be simplified by scaling the multidimensional space by the inverse of the within-group variation, which is equivalent to transforming the whole

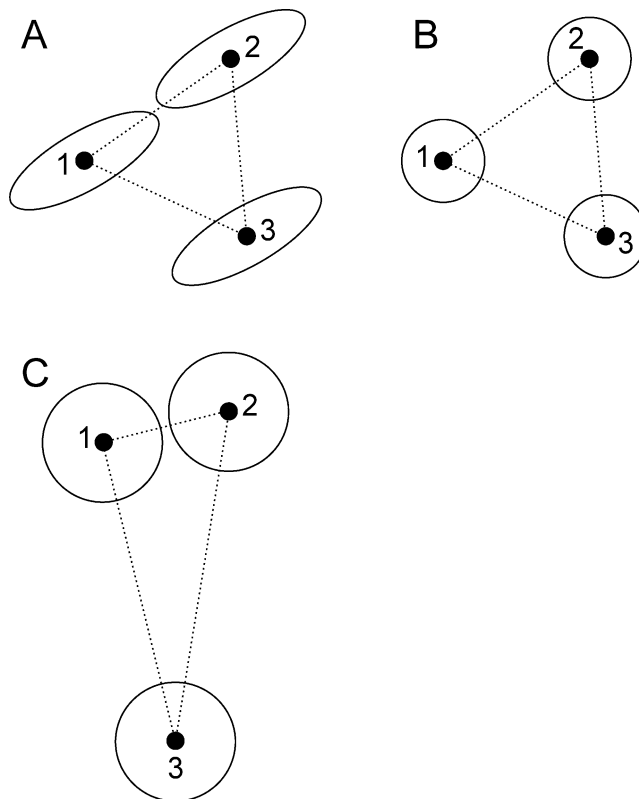


FIGURE 1. Group discrimination and distances. A, Example of three groups with nonisotropic variation. Even though the Euclidean distances between all three group means are equal (the three means form an equilateral triangle), the separation between groups 1 and 2 is less clear than between either one of these and group 3. B, Example of three groups with isotropic variation. All groups are equally separate from each other. C, The example of panel A with the space transformed so that within-group variation becomes isotropic. The distances are transformed from Euclidean to Mahalanobis distances. The three group means no longer form an equilateral triangle.

multivariate space by rotating, stretching, compressing, and shearing so that variation within groups becomes isotropic. Figure 1C shows this transformed space for the situation in Figure 1A and clearly demonstrates that the transformation has a profound effect on the distances between groups. The distances in the transformed space measure the differences between groups relative to the within-group variation, and are known in multivariate statistics as the Mahalanobis distances (e.g., Mardia et al., 1979). These distances directly reflect the degree of separation between groups, and the direction of variation within groups needs not be considered in this space because it is isotropic by definition.

This transformation is a central idea for computing discriminant functions and for canonical variate analysis (e.g., Albrecht, 1980; Campbell and Atchley, 1981; Carroll et al., 1997). The discriminant function between two groups is computed as  $\mathbf{W}^{-1}\mathbf{d}$ , where  $\mathbf{d}$  is the difference vector between the two group means and  $\mathbf{W}^{-1}$  is the inverse of the within-group covariance matrix  $\mathbf{W}$ . The discriminant functions therefore correspond to the lines connecting pairs of group means in Figure 1C, and

discriminant scores are computed by orthogonal projection of the data points onto those lines. Similarly, canonical variate analysis is based on a transformation of the among-group covariance matrix  $\mathbf{B}$  by premultiplying with  $\mathbf{W}^{-1}$ , followed by a principal component analysis of the matrix  $\mathbf{W}^{-1}\mathbf{B}$  (Albrecht, 1980; Campbell and Atchley, 1981). The resulting canonical variates are those variables that account for the maximum amount of among-groups difference relative to the within-group variation. Due to the transformation by  $\mathbf{W}^{-1}$ , the resulting canonical or discriminant space is different from the space of the original variables to the degree that  $\mathbf{W}$  differs from being proportional to an identity matrix. The transformation is more drastic if the variances of the variables greatly differ from each other or if the variables are highly correlated with each other.

Unless the within-group variation of shape is isotropic (i.e.,  $\mathbf{W}$  is proportional to an identity matrix), the process of the transformation by  $\mathbf{W}^{-1}$  will cause some combination of stretching, rotation, and shearing of the multivariate space and thereby alter its geometry so that it does not retain the characteristics of a shape tangent space. Shape tangent spaces have special properties that link their geometry to that of the plane or three-dimensional space in which the landmark configuration has been digitized and in which shapes can be reconstructed graphically (Rohlf, 1999). First, directions that are perpendicular in the original configuration correspond to perpendicular directions in shape tangent space. Second, all the axes within each space are scaled equally. Therefore, any two landmark shifts in configuration space that are equal in magnitude, but which may differ in their direction or occur at different landmarks, will produce shifts of equal magnitude in shape tangent space (for small amounts of shape variation). These two properties are the basis for using Procrustes distances as a metric for shape changes and they ensure that each point in shape tangent space can be visualized directly as a shape.

Stretching and shearing by the transformation with the matrix  $\mathbf{W}^{-1}$  can destroy these properties. The transformation may apply a different scaling factor for each landmark and even for different directions of variation for a single landmark. Moreover, directions that were orthogonal in the original configuration may no longer correspond to orthogonal directions in the transformed shape tangent space. Figure 2 shows an example of this change in a typical example of the type of variation as it is found in many morphometric data sets, shape variation in the *Drosophila* wing. Variation clearly is not isotropic, because the scatters are neither equally large nor circular (Fig. 2A; in addition, variation at different landmarks is interrelated, which cannot be seen in this diagram). A pair of  $x$  and  $y$  coordinate axes is shown at each landmark, and the axes have consistent directions and scaling for all landmarks (Fig. 2A). The transformation by  $\mathbf{W}^{-1}$  has different effects on different landmarks, as can be seen from the changes to the coordinate axes drawn at the landmarks, which differ in their directions and lengths (Fig. 2B). Because there

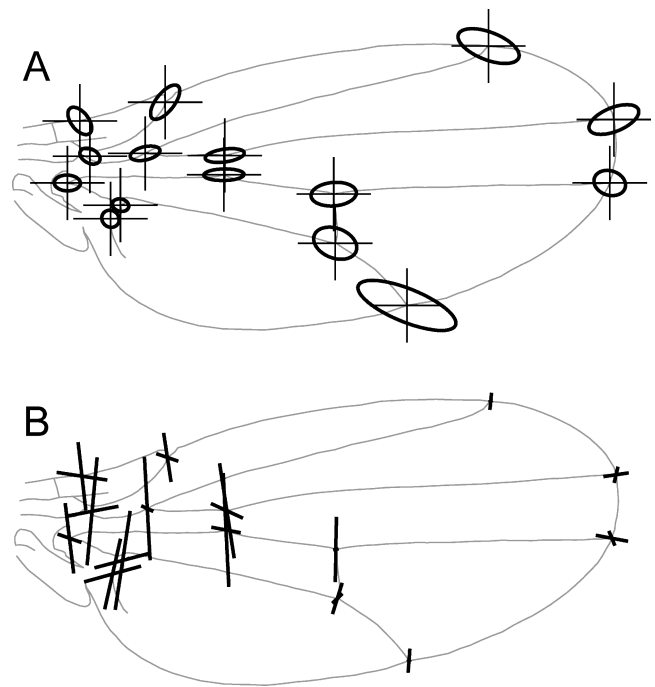


FIGURE 2. Shape variation in the *Drosophila melanogaster* wing and the transformation by  $\mathbf{P}^{-1}$ . A, The patterns of landmark variation in the wing. The ellipses showing the dispersion of landmarks around the Procrustes average have all been magnified by the same factor for better visibility. Note that the landmarks differ in the amount and direction of variation. The  $x$  and  $y$  axes are drawn at each landmark. B, The effects of the transformation by the matrix  $\mathbf{P}^{-1}$  on the coordinate axes for the different landmarks. The coordinate axes from panel A are here shown after the transformation. Notice the unequal scaling and shearing of axes for some of the landmarks. All axes are scaled by the same factor, but they have been superimposed arbitrarily on the locations of the corresponding landmarks in the original configuration (in the transformed space, there is no overall scale for the  $x$  and  $y$  axes as there is in the configuration space). The landmark locations and the transformed axes are not even in the same units (see text). We emphasize, therefore, that this diagram is meant to illustrate the difficulties of presenting the transformed space, but definitely not as a suggested solution!

is no consistent scaling of the coordinates in the transformed space, we chose to construct Figure 2B with the landmark arrangement of the mean shape (this choice is arbitrary, even though it may look deceptively natural). Moreover, the transformed coordinates are in units of the inverse of shape (another reason why the combination with the original landmark configuration in Fig. 2B is problematic). The Procrustes metric and other features of shape tangent space clearly do not apply here and, other than by undoing the transformation altogether, there is therefore no direct or natural relationship from the transformed shape tangent space back to the original configuration.

Transformations of this sort play an important role in applications of morphometric methods to a wide range of different biological problems. In this paper, we will concentrate on two contrasting applications: quantitative genetics, including the analysis of selection on shape, and the measurement of fluctuating asymmetry in shape.

## GEOMETRIC MORPHOMETRICS AND THE MULTIVARIATE THEORY OF QUANTITATIVE GENETICS

A context in which this sort of transformation plays a central role is quantitative genetics, clearly a critical area for understanding the micro- and macroevolution of organismal shape (Felsenstein, 1988, 2002; Stepan et al., 2002). So far, most quantitative genetic studies of shape are univariate analyses of single shape variables derived from landmark or outline analyses, which either use classical quantitative genetic approaches (e.g., Arnqvist and Thornhill, 1998; Currie et al., 2000; Albertson et al., 2003b) or searches for quantitative trait loci (QTLs; e.g., Liu et al., 1996; Zimmerman et al., 2000; Albertson et al., 2003a). These analyses are restricted a priori to investigate a single aspect of shape in isolation, and they cannot consider how different shape features may be related to each other. In contrast, studies of the quantitative genetics of shape as a whole, rather than single shape variables, require an explicitly multivariate approach. Such methods have been introduced for QTL analyses (Klingenberg et al., 2001b, 2004; Workman et al., 2002) as well as for classical quantitative genetic approaches (Klingenberg and Leamy, 2001; Monteiro et al., 2002; Fernández Iriarte et al., 2003), but the latter applications have generated some debate (Klingenberg, 2003b; Monteiro et al., 2003).

Klingenberg and Leamy (2001) combined the methods of geometric morphometrics with the standard multivariate theory of quantitative genetics (e.g., Lande, 1979; Cheverud, 1984; Roff, 1997; Lynch and Walsh, 1998). In contrast, Monteiro et al. (2002) used Procrustes distance to define a new scalar measure of heritability for shape, which is the ratio of the amount of genetic shape variation to the total amount of shape variation. Klingenberg (2003b) presented additional algebraic explanations of this method, linking it explicitly to the multivariate theory of quantitative genetics, and pointed out some limitations of the scalar heritability measure. In their reply, Monteiro et al. (2003) raised questions about the sets of variables used to characterize shape, and suggested that the direction and magnitude of shape variation can be treated as separate questions. We will revisit this suggestion here.

Genetic and phenotypic components of variation can be extracted using the standard statistical tools of quantitative genetics (Lynch and Walsh, 1998), for instance the parent-offspring design (Klingenberg and Leamy, 2001) or other types of analyses of variation within and between groups of closely related individuals (Monteiro et al., 2002; Fernández Iriarte et al., 2003). These analyses yield estimates of the phenotypic covariance matrix  $\mathbf{P}$  and the genetic covariance matrix  $\mathbf{G}$ , which are used in the further analyses. For genetic analyses of shape, the  $\mathbf{P}$  and  $\mathbf{G}$  matrices characterize the entire genetic and phenotypic shape variation, including magnitude and directionality in all the dimensions of the shape tangent space.

The  $\mathbf{G}$  and  $\mathbf{P}$  matrices can be used to predict the complete selection response, both magnitude and direction, with the multivariate version of the breeders' equation

$\Delta\boldsymbol{\mu} = \mathbf{G}\mathbf{P}^{-1}\mathbf{s}$  (Lande, 1979). In this equation,  $\Delta\boldsymbol{\mu}$  is the response to selection, the change in mean shape between the parental and offspring generations, and  $\mathbf{s}$  is the selection differential, the difference between the mean shape in the parental generation and the mean shape of the individuals selected to produce the offspring generation (or the covariance between shape and fitness). Both  $\Delta\boldsymbol{\mu}$  and  $\mathbf{s}$  are vectors in the shape tangent space, and as long as the complete shape information is included in the  $\mathbf{G}$  and  $\mathbf{P}$  matrices, the analyses do not impose any artificial restrictions on the results. Figure 3 provides a simple example of this kind of analysis for two dimensions (the shape tangent space for a triangle of landmarks), showing that the direction of  $\mathbf{s}$  and  $\Delta\boldsymbol{\mu}$  may not be the same and that the magnitude of  $\Delta\boldsymbol{\mu}$  also depends on the specific  $\mathbf{s}$  used (Fig. 3B, C).

The geometric reasoning that underlies the multivariate theory of quantitative genetics is similar to the transformations explained above for discriminant analysis. The multivariate breeders' equation,  $\Delta\boldsymbol{\mu} = \mathbf{G}\mathbf{P}^{-1}\mathbf{s}$ , can be viewed as consisting of two sequential transformation steps, in which the original selection differential  $\mathbf{s}$  is changed into the response to selection  $\Delta\boldsymbol{\mu}$  (Lande, 1979). In the first transformation, the selection differential is premultiplied by the inverse of the phenotypic covariance matrix, which transforms it into the selection gradient,  $\boldsymbol{\beta} = \mathbf{P}^{-1}\mathbf{s}$ . The transformation by  $\mathbf{P}^{-1}$  yields a new trait space in which the phenotypic variation is isotropic, eliminating the effects of phenotypic covariation, and therefore the selection gradient reflects the direct effects of selection on the traits. The selection gradient is a vector of partial regression coefficients of relative fitness on the phenotypic variables (Lande and Arnold, 1983; Phillips and Arnold, 1989). The second transformation, this one using the  $\mathbf{G}$  matrix, relates the within-generation effects of selection to the response in the following generation,  $\Delta\boldsymbol{\mu} = \mathbf{G}\boldsymbol{\beta}$ . In a way, the transformation by  $\mathbf{G}$  is the reverse of the transformation by  $\mathbf{P}^{-1}$ , as it projects the vector of selection effects from the space of partial effects back to the original shape tangent space, but it uses the additive genetic covariance matrix because this mapping is from the parental to the offspring generation. In the juxtaposition of both these transformation steps as parts of the multivariate breeders' equation, both the phenotypic and genetic covariance structures play a role, and together they can produce results that may appear counterintuitive at first (e.g., Fig. 3).

### *Magnitude and Direction: Are They Really Separable?*

A key point emphasized by Monteiro et al. (2003) is that the magnitude and direction of shape change are questions that can be treated separately. Accordingly, it should be possible to use the univariate breeders' equation with the shape heritability  $h^2$  to predict the magnitude of the selection response from the magnitude of the selection differential (Monteiro et al., 2002: 569), or using the notation above,  $\|\Delta\boldsymbol{\mu}\| = h^2\|\mathbf{s}\|$ , where the double bars denote the length of the respective vector. The

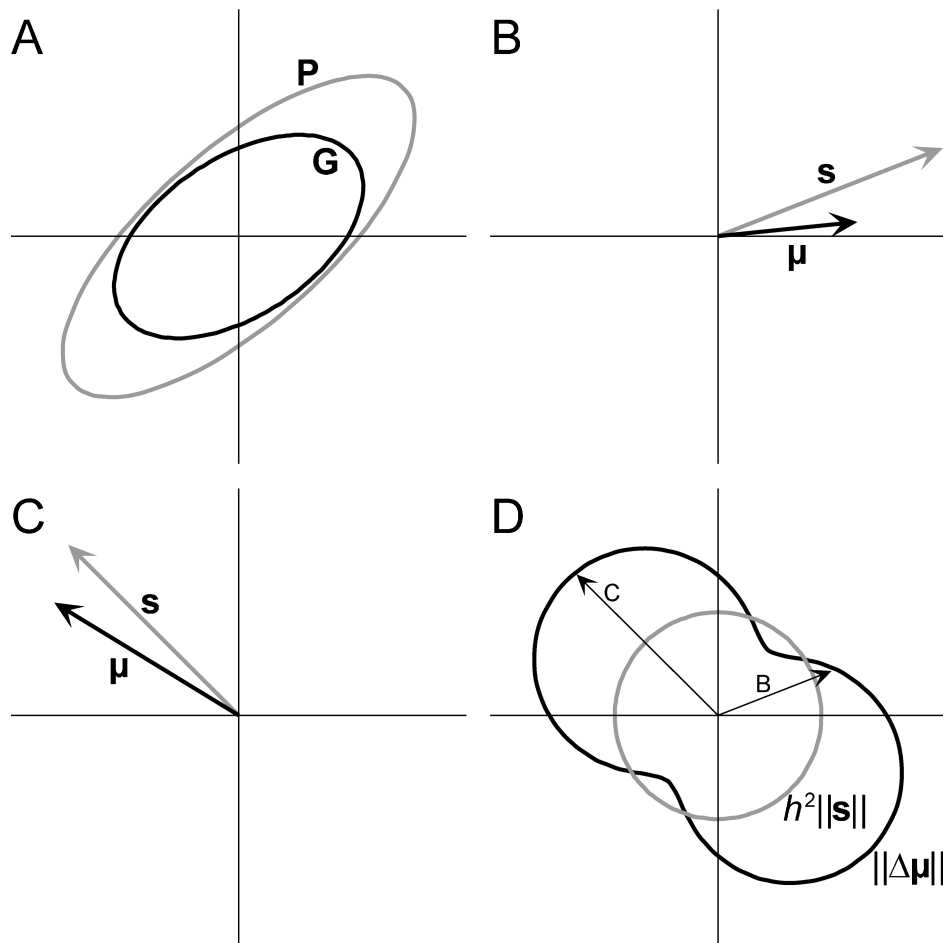


FIGURE 3. Simulation of selection in different directions in two dimensions (e.g., the tangent space for shape variation in a triangle of landmarks). A, Contours illustrating the magnitude and directionality of variation in the additive genetic covariance matrix **G** (black ellipse) and the phenotypic covariance matrix **P** (gray ellipse) used in this example. B, C, Selection with two different selection differentials. In each panel, **s** is the selection differential (gray arrow) and  $\Delta\mu$  is the response to selection. D, Polar plots of the predicted magnitude of the selection response as a function of the direction of the selection differential (the magnitude of the selection response, graphed in the direction of the selection differential). The black figure shows the magnitude of the response  $\|\Delta\mu\|$  predicted by the multivariate breeders' equation (Lande, 1979), which considers both the amount and direction of variation jointly. The gray circle indicates the magnitude  $h^2\|s\|$  predicted using the univariate breeders' equation and the shape heritability  $h^2$  according to Monteiro et al. (2002). The arrows labeled B and C indicate the points corresponding to the examples shown in panels B and C. Note that the coordinate system in the polar plot of panel D is not the same as in panels A to C, which represent the shape tangent space.

shape heritability of Monteiro et al. (2002) can be computed as the total variance of **G** divided by the total variance of **P** (the sum of the diagonal elements of **G** divided by the sum of the diagonal elements of **P**). This approach differs from the one outlined in the previous section in that it does not consider the direction of the selection differential and the directionality of variation in **G** and **P**.

To illustrate the differences between the two approaches, we present a simple simulation in two dimensions, which might be the shape tangent space for a triangle of landmarks. The simulation used the following **G** and **P** matrices (in arbitrary units; Fig. 3A):

$$\mathbf{G} = \begin{bmatrix} 3 & 1.2 \\ 1.2 & 2 \end{bmatrix} \quad \text{and} \quad \mathbf{P} = \begin{bmatrix} 6 & 4 \\ 4 & 5 \end{bmatrix}.$$

The shape heritability (Monteiro et al., 2002) can therefore be calculated as the ratio of the total variances of the **G** and **P** matrices,  $h^2 = 5/11 = 0.45$ . Using this estimate and the univariate breeders' equation, the predicted magnitude of the selection response would therefore be 0.45 times the magnitude of the selection differential, *regardless of the direction* of selection (Monteiro et al., 2002: 569).

The simulations with the multivariate breeders' equation are shown for two selection differentials, both of the same length, but with different directions (Fig. 3B, C, gray arrows labeled **s**). Both the directions and the magnitudes of the responses to selection differ between the two simulations (black arrows labeled  $\Delta\mu$ ). We repeated this simulation for selection in all possible directions, and we graphed the magnitudes of the predicted responses against the direction of the selection differential as polar

plots (Fig. 3D). Because the same magnitude of response is expected for the shape heritability approach, the resulting plot is a circle (gray circle labeled  $h^2||s||$ ). In contrast, the polar plot for the magnitude of the response predicted by the multivariate breeders' equation is a more irregular shape somewhat resembling a peanut (black figure labeled  $||\Delta\mu||$ ), which indicates that the magnitude of the selection response changes markedly according to the direction of the selection differential. As can easily be seen, the two estimates of the magnitude of selection response differ substantially.

This simulation also shows that the estimate based on shape heritability need not even provide a good estimate for the average of the selection response computed with the multivariate breeders' equation. For most directions of the selection differential, the estimate based on shape heritability substantially underestimates the magnitude of the response (Fig. 3D). Considering the direction of selection is therefore essential for predicting the magnitude of the response. This example shows that magnitude and direction are not separate questions, but are tightly interlinked and should be considered jointly in quantitative genetic studies of shape. We conclude that careful attention should be paid to the stringent assumptions implicit in the shape heritability of Monteiro et al. (2002) and that it should be used only if variation is isotropic or if the  $\mathbf{P}$  and  $\mathbf{G}$  matrices are proportional (Klingenberg, 2003b). We would like to remind readers that a significant matrix correlation between the  $\mathbf{P}$  and  $\mathbf{G}$  matrix, as it can be obtained by a matrix permutation test (Mantel test, e.g., Mantel, 1967; Cheverud et al., 1989; Klingenberg and McIntyre, 1998) does not necessarily indicate proportionality. If the  $\mathbf{P}$  and  $\mathbf{G}$  matrices are proportional, then the matrix  $\mathbf{G}\mathbf{P}^{-1}$  will be a scalar multiple of the identity matrix (all off-diagonal entries zero and all diagonal entries equal). This is a better criterion to assess whether the  $\mathbf{G}$  and  $\mathbf{P}$  matrices are sufficiently proportional for the use of the scalar shape heritability.

#### *Interpreting and Visualizing Multivariate Selection on Shape*

The two alternative descriptors of linear selection,  $\mathbf{s}$  and  $\beta$ , differ in a number of ways that are consequences of the transformation of  $\mathbf{s}$  by  $\mathbf{P}^{-1}$ . The selection differential  $\mathbf{s}$  is the vector of covariances between fitness and the shape variables, or the difference of phenotypic means in the parental generation before and after selection (e.g., Lande and Arnold, 1983; Falconer and Mackay, 1996: chapter 11). The selection differential also corresponds to the shape variable that can be extracted by a partial least squares analysis (Rohlf and Corti, 2000) of the covariation between shape and fitness. Overall, the selection differential is a descriptor of the total effect of selection, but it does not distinguish between direct and indirect selection and does therefore not provide information about the agency of selection.

If the causal basis of selection on shape is of interest, the selection gradient  $\beta$  may be the appropriate descriptor, because it is the vector of the multiple regression

coefficients of fitness on shape. For each shape variable, this estimate partials out the effect of all other aspects of shape on fitness. It therefore represents the direct effect of each variable on fitness separately, and corrects for indirect selection.

In the context of geometric morphometrics, however, these interpretive advantages come at a cost, because they eliminate the possibility for direct visualization. The selection differential is a shape change, but the selection gradient is not (it is in units of the inverse of shape). The selection differential can be calculated directly as the difference in mean shape before and after selection (for threshold selection; Falconer and Mackay, 1996: chapter 11) or as the covariance of shape with relative fitness, which is dimensionless (Lande and Arnold, 1983). Selection differentials therefore are vectors in shape tangent space and can be visualized directly with the graphical tools customary in geometric morphometrics (Klingenberg and Leamy, 2001). The transformation of  $\mathbf{s}$  to the selection gradient  $\beta$  by the matrix  $\mathbf{P}^{-1}$  changes its nature, so that it is no longer a vector in shape tangent space. All the problems of interpretation outlined above therefore apply to the selection gradient with full severity.

In particular, selection gradients should not be visualized as shape changes (like the coordinate axes in Fig. 2B), tempting and apparently intuitive as this may appear at first sight. Instead, the method for visualizing the shape features associated with selection should follow the procedure used, for example, for canonical variate analysis (Rohlf et al., 1996: 354). The method consists of a multivariate regression of the shape variables (Procrustes residuals or partial warp scores and uniform components) on the canonical variate scores, which yields the expected shapes of specimens with low and high canonical variate scores. In the context of natural selection, the analogue of this approach is to visualize the expected shapes of individuals with high or low fitness. The procedure is to compute a predicted fitness score for each individual by multiplying its shape variables by the selection gradient  $\beta$ . The multivariate regression of shape on this fitness score yields a vector of regression coefficients that can be visualized directly. This vector is directly proportional to the selection differential  $\mathbf{s}$ , with a scaling factor equal to the reciprocal of the variance of the fitness score (in essence, the multivariate regression has undone the transformation from  $\mathbf{s}$  to  $\beta$ ). An equivalent solution, with a resulting shape variable that is a scaled version of  $\mathbf{s}$ , can be obtained from a partial least squares analysis of shape and fitness (Rohlf and Corti, 2000). To put it simply, the rule in geometric morphometric studies of selection on shape is to display selection differentials and not selection gradients.

#### A MODIFIED SHAPE DISTANCE FOR NON-ISOTROPIC VARIATION

The ideas about transformed spaces are applicable not only in quantitative genetics. Here we use them in a contrasting biological context to formulate a modified shape

distance that quantifies the magnitude of shape differences relative to the variation in a sample.

An application of this shape distance is fluctuating asymmetry, which is thought to originate from random perturbations in development (Palmer and Strobeck, 1986; Møller and Swaddle, 1997; Klingenberg, 2003a). Because it is of random origin, an individual's deviation from symmetry could have any direction, which is often of little biological interest. The magnitude of the deviation, however, is modulated by the developmental system, which in turn may respond to factors such as environmental stress or the genotype (Palmer and Strobeck, 1986; Møller and Swaddle, 1997; Klingenberg and Nijhout, 1999). To investigate these effects, the magnitude of asymmetry is a sufficient measure of individual asymmetry, whereas the direction of individual asymmetry is normally not of interest.

For studies of fluctuating asymmetry and other situations where the direction of the effects in particular individuals is of no biological interest, we propose a distance measure that can provide a scalar measure of the relative extent of shape differences, while taking into account that variation may not be isotropic. This distance measure is based on the idea of one-sample standard distance (Flury and Riedwyl, 1986; Flury, 1997), which is equivalent to the one-sample version of the Mahalanobis distance (Mardia et al., 1979: 31). Note, however, that the full shape change cannot be reconstructed from such a distance measure alone and that no visualization as a shape change is therefore possible.

The computation of this distance involves a transformation of the original space (Fig. 4A) to a space in which the variation is isotropic (Fig. 4B). The distances are then computed as Euclidean distances in the transformed space and can be compared without reference to the directions of the original deviations (Fig. 4C). The transformation step changes the geometry of the space, both in terms of directions and distances (arrows in Fig. 4), but it maintains the magnitude of each individual deviation *relative to* the amount of sample variation in that direction. Because the variation after transformation is the same in every direction, the information about directions then can be dropped and the distances can be directly compared (Fig. 4C).

There are several methods for the computation of the shape deviations from the mean. In compact matrix notation, we can start with an  $n \times p$  matrix  $\mathbf{X}$  that contains the data, for example, the signed shape asymmetries, centered so that all the column means are zero ( $n$  is the sample size and  $p$  is the number of variables in  $\mathbf{X}$ ). Then the covariance matrix can be computed as  $\mathbf{S} = 1/n \mathbf{X}^T \mathbf{X}$ , where the superscript T denotes the matrix transpose. The shape distances of each specimen to the mean are then found by taking the square roots of the values on the diagonal of the matrix  $\mathbf{X} \mathbf{S}^{-1} \mathbf{X}^T$ , where  $\mathbf{S}^{-1}$  is the generalized inverse of  $\mathbf{S}$ .

An equivalent calculation of these distances can be done easily with standard statistics software using the following procedure: (1) carry out a principal compo-

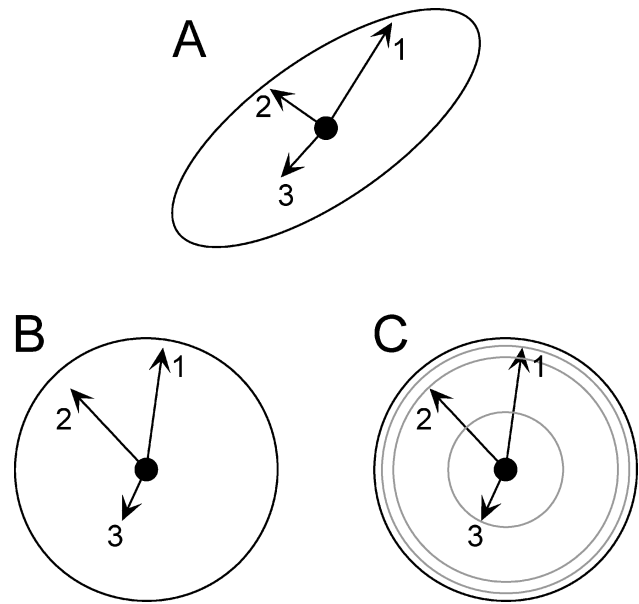


FIGURE 4. A modified distance measure for shape deviations, for instance fluctuating asymmetry, in the presence of nonisotropic variation. A, Original distribution of shape deviations around their average. Three individual cases, drawn haphazardly from the distribution, are shown as numbered arrows. B, After transformation by the inverse of the covariance matrix, the variation around the mean is isotropic and the scatter of data points is transformed from an ellipse into a circle. After the transformations, the directions and lengths of the deviations have changed, but each one has maintained its magnitude relative to the variation in its particular direction. C, The distance from the mean as a relative measure of shape distance. Because variation is isotropic after transformation, the relative magnitudes can be compared directly among shape differences with different directions (gray circles). The distances in the transformed space can therefore be used as a relative measure of shape difference.

nent analysis (using the covariance matrix) of the data, for instance the signed right-left differences of landmark positions, and compute the principal component scores for each observation; (2) standardize the scores for each principal component to variance 1.0; (3) sum up the squares of these standardized principal component scores for every observation; and (4) compute the square root of the resulting sum for each observation. If the analysis is based on partial warps scores and the uniform components of shape variation, all the variables should be included in this procedure, but if the coordinates of Procrustes-superimposed landmarks or Procrustes residuals are used, the last four (for two-dimensional data) or seven (for three-dimensional data) principal components should be omitted from steps (2) to (4) because they have zero variances (up to rounding errors).

The procedure described above can be used with data that are the signed right-left differences of shape (Klingenberg and McIntyre, 1998; Auffray et al., 1999; Klingenberg et al., 2002). Computing the principal components of individual asymmetry vectors from centered data, the default option in most statistics programs, automatically provides a correction for directional

asymmetry, which is almost ubiquitous for shape data (Smith et al., 1997; Klingenberg et al., 1998).

The resulting asymmetry measure takes into account that fluctuating asymmetry is usually nonisotropic (Klingenberg and McIntyre, 1998; Debat et al., 2000; Klingenberg and Zaklan, 2000; Klingenberg et al., 2002), and it is therefore preferable over the individual asymmetry measures based on Procrustes distance (Smith et al., 1997; Klingenberg and McIntyre, 1998). Moreover, because this measure is scalar, and therefore is amenable to univariate statistical analyses, it is considerably simpler than the vector-valued measure of unsigned asymmetry used by Klingenberg et al. (2001b).

We demonstrate this measure of shape distance with an example of fluctuating asymmetry in samples of *Drosophila melanogaster* males from the Oregon-R wild-type strain ( $n = 98$ ) and from a strain heterozygous for the *spalt-major*<sup>1</sup> mutation (*salm*<sup>1</sup>;  $n = 108$ ). The data set includes the coordinates of 15 landmarks (see Fig. 2) on each wing. The landmark configurations for the left wings were reflected, and the shape information for all wings was extracted by Procrustes superimposition. Signed asymmetries were computed as the coordinate differences of the left and right wings of each individual. Preliminary analyses suggested that measurement error was small relative to fluctuating asymmetry.

The variation among the eigenvalues of the covariance matrix of the signed asymmetry clearly indicates that the variation is not isotropic (Fig. 5A). Much of the variation is concentrated in the first few principal components, and the eigenvalues drop markedly before tapering off to small values. The last four eigenvalues are zero because of the four degrees of freedom lost in the Procrustes superimposition for variation in size, position, and orientation. For comparison, we also show the eigenvalues for a simulated data set with isotropic variation and the same sample size (gray line in Fig. 5A). This simulation shows a much more even distribution of the variation over the 26 dimensions.

The plot of the first two principal component scores of the signed asymmetries shows no evident difference in the scatter between the wild-type and mutant flies (Fig. 5B). Also note that the clear anisotropy of the data is not very apparent from this plot, which is a reminder that a nearly circular scatter of principal component scores does not imply isotropic variation.

To compare the degree of asymmetry between the two samples, we computed a score for the asymmetry of wing shape for each fly, using the modified shape distance. The histograms of the asymmetry scores (Fig. 5C) show only a slight difference between the two samples, with the scores for fluctuating asymmetry being slightly higher in the wild-type flies than in the *salm*<sup>1</sup> mutant flies. The difference of the means of 0.56 is statistically significant ( $P = 0.0003$  in a two-tailed permutation test with 10,000 random permutations). This example shows that this measure of asymmetry can pick out relatively subtle differences in the amounts of asymmetry. This will be particularly useful in contexts such as studies of quantitative genetics, where subtle effects are often found. This

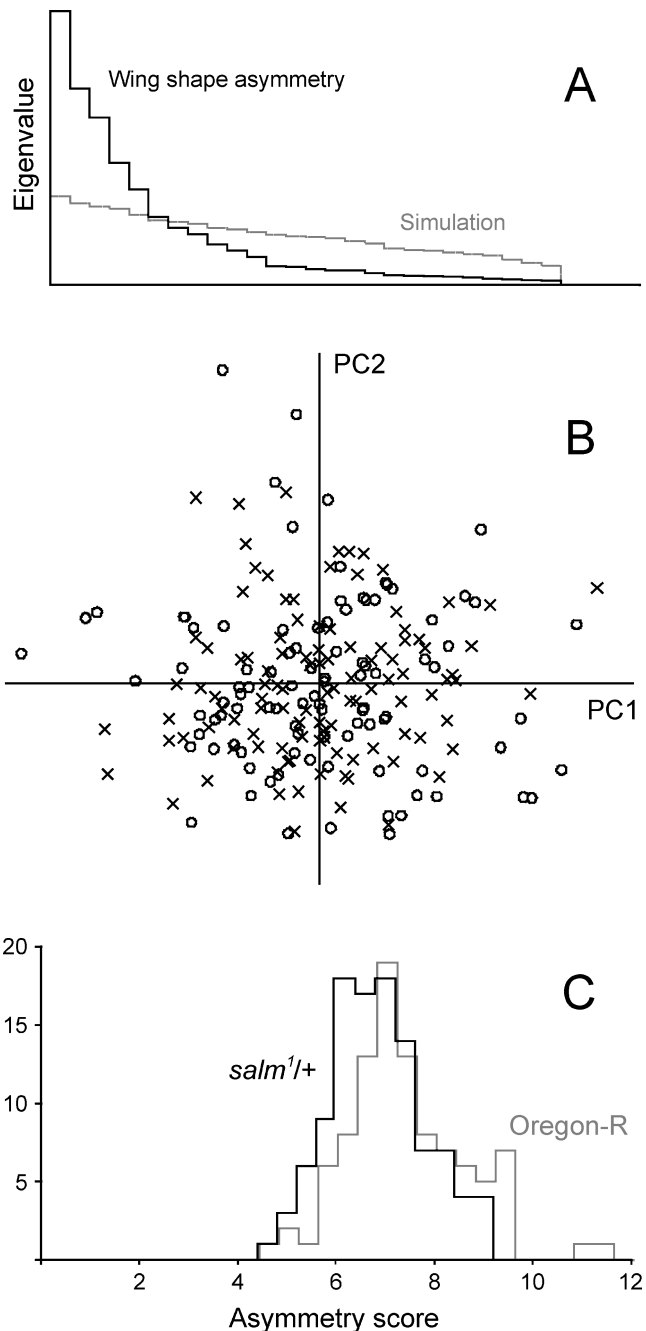


FIGURE 5. Application of the measure of relative shape distance to fluctuating asymmetry of *Drosophila* wings. (A) Eigenvalues of the covariance matrix for fluctuating asymmetry (black histogram) in comparison to a simulated data set drawn from an isotropic distribution (gray histogram). (B) Scatter plot of the scores for the first two principal components for asymmetry. Crosses indicate individuals with *salm*<sup>1</sup>/*+* genotype and circles represent wild-type individuals. (C) Histograms of the asymmetry scores. Scores were computed using the measure of relative shape distance.

scalar measure of shape distance has been applied in a study of the genetic architecture of fluctuating asymmetry in mice (Leamy et al., 2005).

The use of this distance measure for individual asymmetry is made possible by the random origin of

fluctuating asymmetry. This situation is quite different from that in most other applications of geometric morphometrics. For instance, in quantitative genetics of shape, the directionality does matter because genes contribute to an individual's deviation from the population average by some amount in a particular direction. This directionality is shared by individuals carrying the same alleles at a locus, and this shared directionality is responsible for the correlation of phenotypic traits among relatives (Fisher, 1918; Falconer and Mackay, 1996; Lynch and Walsh, 1998). Likewise, in phylogenetic comparative analyses, the deviations are inherited from ancestors to descendants, and the directionality of the deviation from the overall mean therefore tends to be shared among related taxa (Felsenstein, 1988, 2002). In both these examples, it is this shared directionality that causes related individuals or taxa to resemble each other in their morphological features and not just in the amount of difference from the overall average size and shape.

#### CONCLUSIONS

This paper has highlighted the importance of taking nonisotropic variation into account in geometric morphometrics. For instance, in phylogenetic comparative studies of shape (Rohlf, 2002), the anisotropic nature of shape variation is often the very target of morphometric studies that identify the shape features evolving the most or the least to characterize evolutionary trends or stasis and constraints. Likewise, in studies of morphological integration, the focus of interest is the covariation among landmarks (e.g., Badyaev and Foresman, 2000; Klingenberg and Zaklan, 2000).

Here we have particularly stressed the example of quantitative genetic analyses of shape, where the direction of selection will have an effect on both the magnitude and direction of the selection response unless the **G** and **P** matrices are proportional (Klingenberg, 2003b), and direction and magnitude of changes cannot be treated as separate questions. Because of nonisotropic variation the transformation from the selection differential to the selection gradient distorts the geometry of the multivariate space so that it no longer has the properties of a shape tangent space. As a consequence, the selection gradient is not a shape change and therefore cannot be visualized directly. Instead, graphs of the selection differential (showing the shapes corresponding to high or low fitness) should be used to visualize selection.

We also have outlined a contrasting application, for fluctuating asymmetry of shape, where the direction of shape deviations is not of biological interest. This is because the perturbations that cause fluctuating asymmetry are of random origin. The benefit of ignoring the direction is that a scalar measure of the amount of shape asymmetry can be derived, which can be further studied with univariate methods and therefore simplifies the analyses.

Both these applications use, in very different ways, the same framework of transformations of shape spaces and the relationships between Procrustes distance and Mahalanobis distance. This framework is by no means limited to these specific cases, but should be equally applicable

to a broad range of morphometric analyses in different biological contexts.

#### ACKNOWLEDGMENTS

We thank David Houle, Larry Leamy, and Jim Rohlf for discussions that contributed to the development of this paper, and we are grateful to Tim Cole, Jim Rohlf, Norm MacLeod, and Rod Page for comments on a previous version of the manuscript. The work of LRM is supported by grants and research fellowships from Fundação de Amparo a Pesquisa do Estado do Rio de Janeiro (FAPERJ) and Conselho Nacional de Desenvolvimento Científico e Tecnológico (CNPq), and the research of CPK is supported by the Biotechnology and Biological Sciences Research Council, the Leverhulme Trust, the Royal Society, and the Wellcome Trust.

#### REFERENCES

- Albrecht, G. H. 1980. Multivariate analysis and the study of form, with special reference to canonical variate analysis. *Am. Zool.* 20:679–693.
- Arnqvist, G., and R. Thornhill. 1998. Evolution of animal genitalia: Patterns of phenotypic and genotypic variation and condition dependence of genital and non-genital morphology in water strider (Heteroptera: Gerridae: Insecta). *Genet. Res.* 71:193–212.
- Auffray, J.-C., V. Debat, and P. Alibert. 1999. Shape asymmetry and developmental stability. Pages 309–324 *in* On growth and form: Spatio-temporal pattern formation in biology (M. A. J. Chaplain, G. D. Singh, and J. C. McLachlan, eds.). Wiley, Chichester.
- Badyaev, A. V., and K. R. Foresman. 2000. Extreme environmental change and evolution: Stress-induced morphological variation is strongly concordant with patterns of evolutionary divergence in shrew mandibles. *Proc. R. Soc. Lond. B Biol. Sci.* 267:371–377.
- Bookstein, F. L. 1991. Morphometric tools for landmark data: Geometry and biology. Cambridge University Press, Cambridge.
- Bookstein, F. L. 1996. Biometrics, biomathematics and the morphometric synthesis. *Bull. Math. Biol.* 58:313–365.
- Bookstein, F. L. 1998. A hundred years of morphometrics. *Acta Zool. Acad. Sci. Hung.* 44:7–59.
- Bookstein, F. L., P. Gunz, P. Mitteroecker, H. Prossinger, K. Schaefer, and H. Seidler. 2003. Cranial integration in *Homo*: Singular warps analysis of the midsagittal plane in ontogeny and evolution. *J. Hum. Evol.* 44:167–187.
- Campbell, N. A., and W. R. Atchley. 1981. The geometry of canonical variate analysis. *Syst. Zool.* 30:268–280.
- Cardini, A. 2003. The geometry of the marmot (Rodentia: Sciuridae) mandible: Phylogeny and patterns of morphological evolution. *Syst. Biol.* 52:186–205.
- Carroll, J. D., P. E. Green, and A. Chaturvedi. 1997. Mathematical tools for applied multivariate analysis. Academic Press, San Diego.
- Cheverud, J. M. 1984. Quantitative genetics and developmental constraints on evolution by selection. *J. Theoret. Biol.* 110:155–171.
- Cheverud, J. M., G. P. Wagner, and M. M. Dow. 1989. Methods for the comparative analysis of variation patterns. *Syst. Zool.* 38:201–213.
- Corti, M., and F. J. Rohlf. 2001. Chromosomal speciation and phenotypic evolution in the house mouse. *Biol. J. Linn. Soc.* 73:99–112.
- Currie, A. J., S. Ganeshanandam, D. A. Noiton, D. Garrick, C. J. A. Shelbourne, and N. Oraguzie. 2000. Quantitative evaluation of apple (*Malus × domestica* Borkh.) fruit shape by principal component analysis of Fourier descriptors. *Euphytica* 111:219–227.
- Debat, V., P. Alibert, P. David, E. Paradis, and J.-C. Auffray. 2000. Independence between developmental stability and canalization in the skull of the house mouse. *Proc. R. Soc. Lond. B Biol. Sci.* 267:423–430.
- Debat, V., M. Bégin, H. Legout, and J. R. David. 2003. Allometric and nonallometric components of *Drosophila* wing shape respond differently to developmental temperature. *Evolution* 57:2773–2784.
- Dobigny, G., M. Baylac, and C. Denys. 2002. Geometric morphometrics, neural networks and diagnosis of sibling *Taterillus* species (Rodentia, Gerbillinae). *Biol. J. Linn. Soc.* 77:319–327.

- Douglas, M. E., M. R. Douglas, J. M. Lynch, and D. M. McElroy. 2001. Use of geometric morphometrics to differentiate *Gila* (Cyprinidae) within the upper Colorado River basin. *Copeia* 2001:389–400.
- Dryden, I. L., and K. V. Mardia. 1998. *Statistical shape analysis*. Wiley, Chichester.
- Duarte, L. C., L. R. Monteiro, F. J. Von Zuben, and S. F. Dos Reis. 2000. Variation in mandible shape in *Trichomys apereoides* (Mammalia: Rodentia): Geometric analysis of a complex morphological structure. *Syst. Biol.* 49:563–578.
- Falconer, D. S., and T. F. C. Mackay. 1996. *Introduction to quantitative genetics*, 4th edition. Longman, Essex.
- Felsenstein, J. 1988. Phylogenies and quantitative characters. *Annu. Revi. Ecol. Syst.* 19:455–471.
- Felsenstein, J. 2002. Quantitative characters, phylogenies, and morphometrics. Pages 27–44 in *Morphology, shape and phylogeny* (N. MacLeod, and P. L. Forey, eds.). Taylor & Francis, London.
- Fernández Iriarte, P., W. Céspedes, and M. Santos. 2003. Quantitative-genetic analysis of wing form and bilateral asymmetry in isochromosomal lines of *Drosophila subobscura* using Procrustes methods. *J. Genet.* 82:95–113.
- Fisher, R. A. 1918. The correlation between relatives on the supposition of Mendelian inheritance. *Trans. R. Soci. Edinburgh* 52:399–433.
- Flury, B. 1997. *A first course in multivariate statistics*. Springer, New York.
- Flury, B., and H. Riedwyl. 1986. Standard distance in univariate and multivariate analysis. *Am. Stat.* 40:249–251.
- Goodall, C. R. 1991. Procrustes methods in the statistical analysis of shape. *J. R. Stat. Soc. B* 53:285–339.
- Harvati, K. 2003. Quantitative analysis of Neanderthal temporal bone morphology using three-dimensional geometric morphometrics. *Am. J. Phys. Anthropol.* 120:323–338.
- Kent, J. T., and K. V. Mardia. 1997. Consistency of Procrustes estimators. *J. R. Stat. Soc. B* 59:281–290.
- Klingenberg, C. P. 2003a. A developmental perspective on developmental instability: Theory, models and mechanisms. Pages 14–34 in *Developmental instability: Causes and consequences* (M. Polak, ed.) Oxford University Press, New York.
- Klingenberg, C. P. 2003b. Quantitative genetics of geometric shape: Heritability and the pitfalls of the univariate approach. *Evolution* 57:191–195.
- Klingenberg, C. P., A. V. Badyaev, S. M. Sowry, and N. J. Beckwith. 2001a. Inferring developmental modularity from morphological integration: Analysis of individual variation and asymmetry in bumblebee wings. *Am. Nat.* 157:11–23.
- Klingenberg, C. P., M. Barluenga, and A. Meyer. 2002. Shape analysis of symmetric structures: Quantifying variation among individuals and asymmetry. *Evolution* 56:1909–1920.
- Klingenberg, C. P., M. Barluenga, and A. Meyer. 2003a. Body shape variation in cichlid fishes of the *Amphilophus citrinellus* species complex. *Biol. J. Linn. Soc.* 80:397–408.
- Klingenberg, C. P., and L. J. Leamy. 2001. Quantitative genetics of geometric shape in the mouse mandible. *Evolution* 55:2342–2352.
- Klingenberg, C. P., L. J. Leamy, and J. M. Cheverud. 2004. Integration and modularity of quantitative trait locus effects on geometric shape in the mouse mandible. *Genetics* 166:1909–1921.
- Klingenberg, C. P., L. J. Leamy, E. J. Routman, and J. M. Cheverud. 2001b. Genetic architecture of mandible shape in mice: Effects of quantitative trait loci analyzed by geometric morphometrics. *Genetics* 157:785–802.
- Klingenberg, C. P., and G. S. McIntyre. 1998. Geometric morphometrics of developmental instability: Analyzing patterns of fluctuating asymmetry with Procrustes methods. *Evolution* 52:1363–1375.
- Klingenberg, C. P., G. S. McIntyre, and S. D. Zaklan. 1998. Left-right asymmetry of fly wings and the evolution of body axes. *Proc. R. Soc. Lond. B Biol. Sci.* 265:1255–1259.
- Klingenberg, C. P., K. Mebus, and J.-C. Auffray. 2003b. Developmental integration in a complex morphological structure: How distinct are the modules in the mouse mandible? *Evol. Dev.* 5:522–531.
- Klingenberg, C. P., and H. F. Nijhout. 1999. Genetics of fluctuating asymmetry: A developmental model of developmental instability. *Evolution* 53:358–375.
- Klingenberg, C. P., and S. D. Zaklan. 2000. Morphological integration between developmental compartments in the *Drosophila* wing. *Evolution* 54:1273–1285.
- Lande, R. 1979. Quantitative genetic analysis of multivariate evolution, applied to brain: Body size allometry. *Evolution* 33:402–416.
- Lande, R., and S. J. Arnold. 1983. The measurement of selection on correlated characters. *Evolution* 37:1210–1226.
- Leamy, L. J., M. S. Workman, E. J. Routman, and J. M. Cheverud. 2005. An epistatic genetic basis for fluctuating asymmetry of tooth size and shape in mice. *Heredity* 94:316–325.
- Lele, S. R. 1993. Euclidean distance matrix analysis (EDMA): Estimation of mean form and mean form difference. *Math. Geol.* 25:573–602.
- Lele, S. R., and J. T. Richtsmeier. 2001. An invariant approach to statistical analysis of shapes. Chapman & Hall/CRC, Boca Raton.
- Liu, J., J. M. Mercer, L. F. Stam, G. C. Gibson, Z.-B. Zeng, and C. C. Laurie. 1996. Genetic analysis of a morphological shape difference in the male genitalia of *Drosophila simulans* and *D. mauritiana*. *Genetics* 142:1129–1145.
- Lynch, M., and B. Walsh. 1998. *Genetics and analysis of quantitative traits*. Sinauer Associates, Sunderland, Massachusetts.
- Mantel, N. 1967. The detection of disease clustering and a generalized regression approach. *Cancer Res.* 27:209–220.
- Mardia, K. V., J. T. Kent, and J. M. Bibby. 1979. *Multivariate analysis*. Academic Press, London.
- Møller, A. P., and J. P. Swaddle. 1997. *Asymmetry, developmental stability and evolution*. Oxford University Press, Oxford.
- Monteiro, L. R., J. A. F. Diniz-Filho, S. F. Dos Reis, and E. D. Araújo. 2002. Geometric estimates of heritability in biological shape. *Evolution* 56:563–572.
- Monteiro, L. R., J. A. F. Diniz-Filho, S. F. Dos Reis, and E. D. Araújo. 2003. Shape distances in general linear models: Are they really at odds with the goals of morphometrics? A reply to Klingenberg. *Evolution* 57:196–199.
- Palmer, A. R., and C. Strobeck. 1986. Fluctuating asymmetry: Measurement, analysis, patterns. *Annu. Rev. Ecol. Syst.* 17:391–421.
- Palmer, A. R., and C. Strobeck. 2003. Fluctuating asymmetry analyses revisited. Pages 279–319 in *Developmental instability: Causes and consequences* (M. Polak, ed.). Oxford University Press, New York.
- Phillips, P. C., and S. J. Arnold. 1989. Visualizing multivariate selection. *Evolution* 43:1209–1222.
- Roff, D. A. 1997. *Evolutionary quantitative genetics*. Chapman & Hall, New York.
- Rohlf, F. J. 1999. Shape statistics: Procrustes superimpositions and tangent spaces. *J. Classif.* 16:197–223.
- Rohlf, F. J. 2001. Comparative methods for the analysis of continuous variables: Geometric interpretations. *Evolution* 55:2143–2160.
- Rohlf, F. J. 2002. Geometric morphometrics and phylogeny. Pages 175–193 in *Morphology, shape, and phylogeny* (N. MacLeod, and P. L. Forey, eds.). Taylor & Francis, London.
- Rohlf, F. J., and M. Corti. 2000. The use of two-block partial least-squares to study covariation in shape. *Syst. Biol.* 49:740–753.
- Rohlf, F. J., A. Loy, and M. Corti. 1996. Morphometric analysis of Old World Talpidae (Mammalia, Insectivora) using partial-warp scores. *Syst. Biol.* 45:344–362.
- Rüber, L., and D. C. Adams. 2001. Evolutionary convergence of body shape and trophic morphology in cichlids from Lake Tanganyika. *J. Evol. Biol.* 14:325–332.
- Smith, D. R., B. J. Crespi, and F. L. Bookstein. 1997. Fluctuating asymmetry in the honey bee, *Apis mellifera*: Effects of ploidy and hybridization. *J. Evol. Biol.* 10:551–574.
- Steppan, S. J., P. C. Phillips, and D. Houle. 2002. Comparative quantitative genetics: Evolution of the G matrix. *Trends Ecol. Evol.* 17:320–327.
- Workman, M. S., L. J. Leamy, E. J. Routman, and J. M. Cheverud. 2002. Analysis of quantitative trait locus effects on the size and shape of mandibular molars in mice. *Genetics* 160:1573–1586.
- Zimmerman, E., A. Palsson, and G. Gibson. 2000. Quantitative trait loci affecting components of wing shape in *Drosophila melanogaster*. *Genetics* 155:671–683.

First submitted 20 July 2004; reviews returned 22 October 2004;

final acceptance 23 November 2004

Associate Editor: Norm MacLeod